Supplementary Material (ESI) for Dalton Transactions

Supporting Information

Entropically Driven Self-assembly of a Strained Hexanuclear Indium Metal–organic Macrocycle and its Behavior in Solution

Minhak Oh,[a] Xinfang Liu,[ab] Mira Park,[b] Dongwook Kim,[b] Dohyun Moon*[c] and Myoung Soo Lah*[a]

[a] Interdisciplinary School of Green Energy, Ulsan National Institute of Science & Technology, Ulsan, 689-798, Korea

[b] Department of Chemistry and Applied Chemistry, Hanyang University, Ansan, Kyunggi-do, 426-791, Korea

[c] Pohang Accelerator Laboratory, Pohang, Kyungbook 790-784, Korea

mslah@unist.ac.kr

Crystal structure determination

$[In_6(H_2L^4)_6(NO_3)(MeOH)_4(H_2O)](NO_3)_5$, 1

A hexanuclear In–MOM with one nitrate anion and five solvent molecules (four methanol molecules and one water molecule) ligated to three alternating metal ions, five additional nitrate counter anions, and at least six structural solvent sites (four methanol molecules and two statistically disorderd water molecules) were identified as an asymmetric unit. The cyclopentyl residues of two ligands in the MOM were statistically disordered. All non-hydrogen atoms except those in the disoredred residues and a methyl carbon atom of a ligated methanol molecule were refined anisotropically; hydrogen atoms were assigned isotropic displacement coefficients U(H) = 1.2U (C, N) and 1.5U (C_{methyl}), and their coordinates were allowed to ride on their respective atoms. All the hydrogen atoms of the ligated amino groups of the ligands were assumed protonated and their coordinates were allowed to ride on the nitrogen atoms, which were assumed to be in the sp^3-hybridized state. The hydrogen atoms attached to the oxygen atoms of the ligated methanol molecules and attacted to the water molecules were not included in the least-squares refinement. The least-squares refinement of the structural model was performed under various geometry and dispalcement parameter restraints such as SADI, DFIX, DANG, FLAT, SIMU, and ISOR. The refinement converged to a final $R1$ = 0.0554, and $wR2$ = 0.1297 for 11198 reflections with $I > 2\sigma(I)$, $R1$ = 0.0841, $wR2$ = 0.1425, GOF = 0.957 for all 15841 reflections. The largest difference peak and hole were 0.780 and –0.981 e·Å^{-3}, respectively.

$[In_6(H_2L^4)_6(H_2O)_6](NO_3)_6$, 2

One and a half hexanuclear In–MOMs with a half on a crystallographic twofold axis were identified as an asymmetric unit. All of the potential ligated solvent sites in the MOMs are occupied by water molecules (the data quality of the structure does not provide unambiguous identities of the ligated solvent sites as some of them could be either partially identified methanol molecules or nitrate anions). Two additional water sites were identified; both of them were in the center of the hexanuclear In–MOM. Only the heteroatoms were refined anisotropically and the carbon atoms were refined isotropically; hydrogen atoms were assigned isotropic displacement coefficients U(H) = 1.2U (C, N), and their

coordinates were allowed to ride on their respective atoms. All the hydrogen atoms of the ligated amino groups of the ligands were assumed to be protonated and their coordinates were allowed to ride on the nitrogen atoms, which were assumed to be in the sp^3-hybridized state. One cyclopentyl group, non-coordinating nitrate groups, and some coordinating solvent groups of bad geometries were refined with geometry restraints. Because of the limited data quality, the least-squares refinement of the structural model was performed under various geometry and dispalcement parameter restraints such as SADI, DFIX, DANG, FLAT, SIMU, and ISOR. The crystal was assumed to be a racemic twinned structure based on the Flack parameter. The refinement converged to $R1 = 0.1725$ and $wR2 = 0.4311$ for 14585 reflections with $I > 2\sigma(I)$, $R1 = 0.2120$, and $wR2 = 0.4578$ for all 25059 reflections. The structure refinement was further performed after modification of the data for the lattice solvent molecules and the unidentified disordered nitrate anions (10101 $Å^3$, 30.4% of the crystal volume) using the *SQUEEZE* routine of the PLATON software package (Ver. 130605),[10] which led to better refinement and parameter convergence. The refinement converged to a final $R1 = 0.0984$ and $wR2 = 0.2833$ for 14523 reflections with $I > 2\sigma(I)$, $R1 = 0.1263$, $wR2 = 0.3030$, GOF = 1.030 for all 25059 reflections. The largest difference peak and hole were 1.372 and –0.991 $e \cdot Å^{-3}$, respectively.

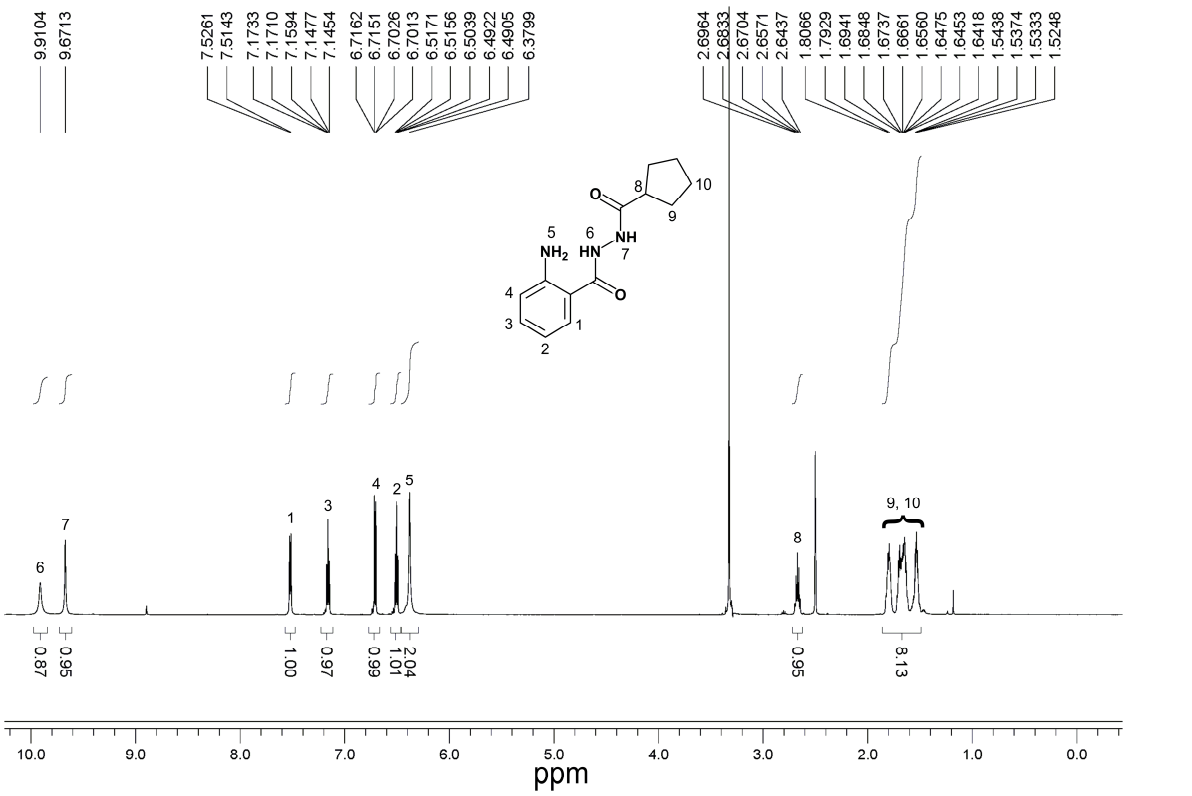

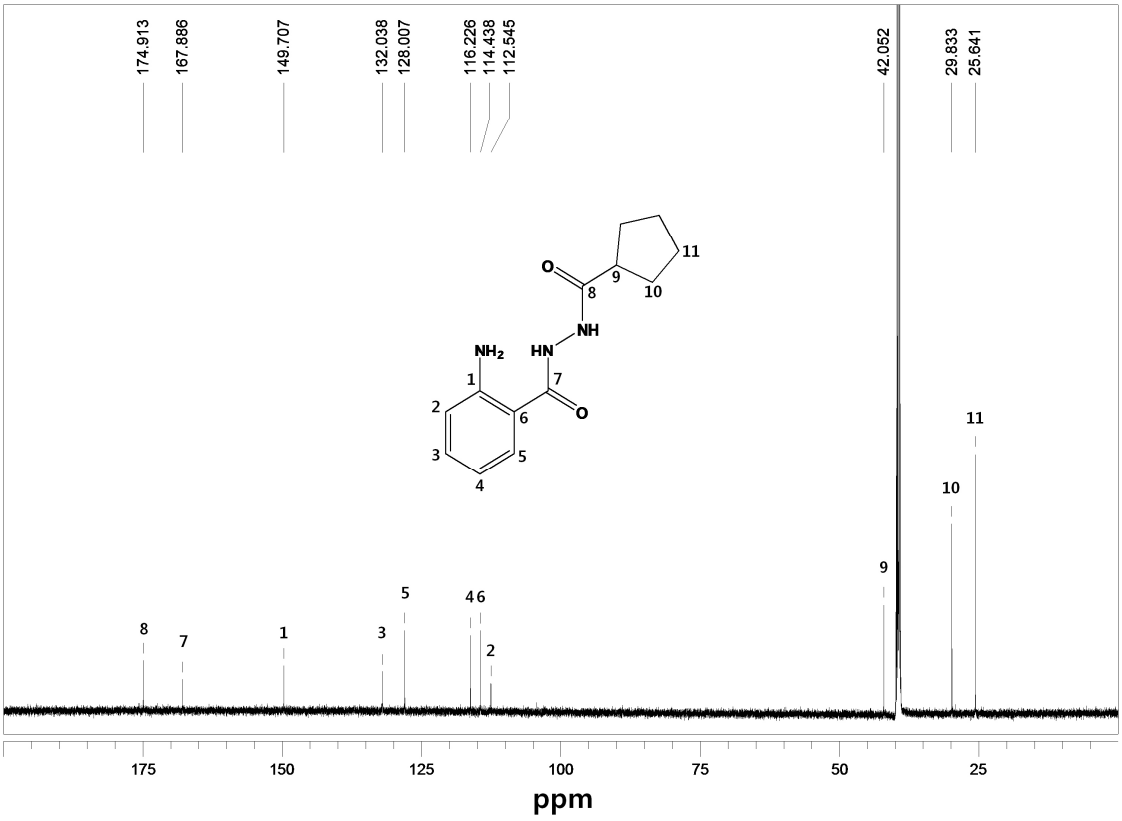

Figure S1. ^{1}H and ^{13}C NMR spectra of H_4L[4].

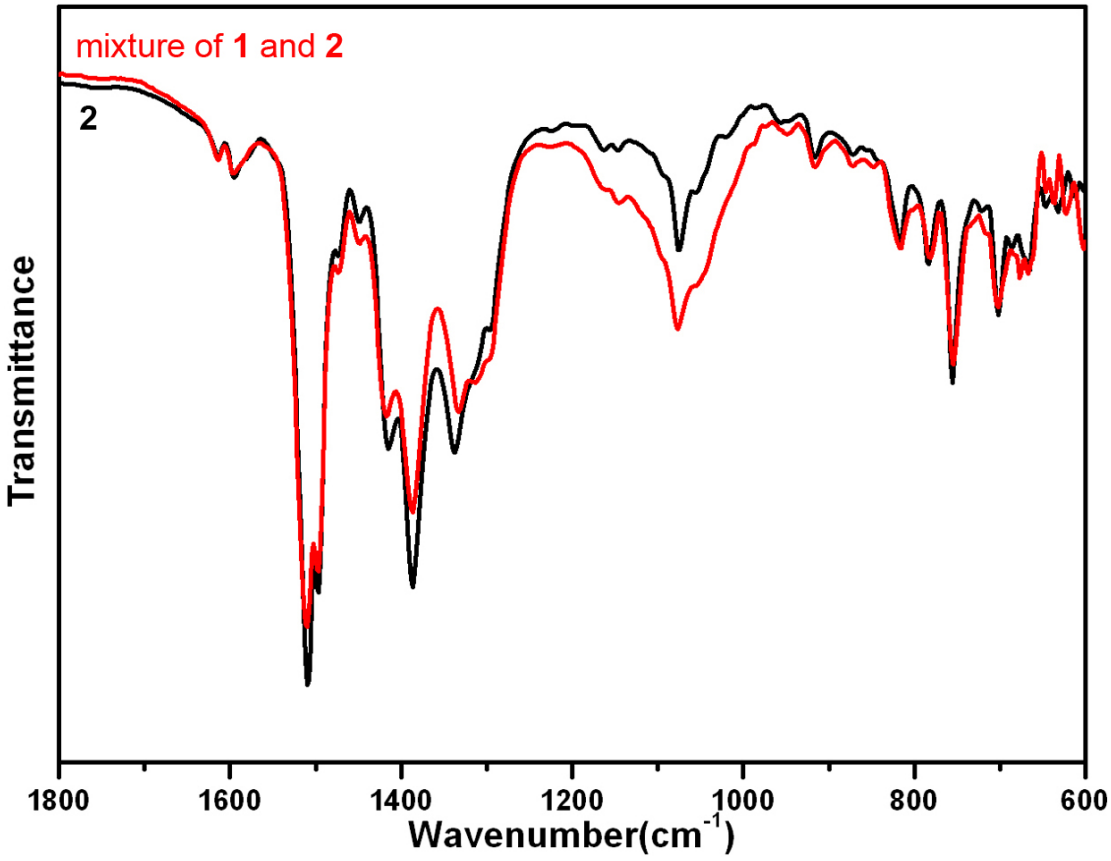

Figure S2. IR spectra of the mixture of **1** and **2** (red) and **2** (black).

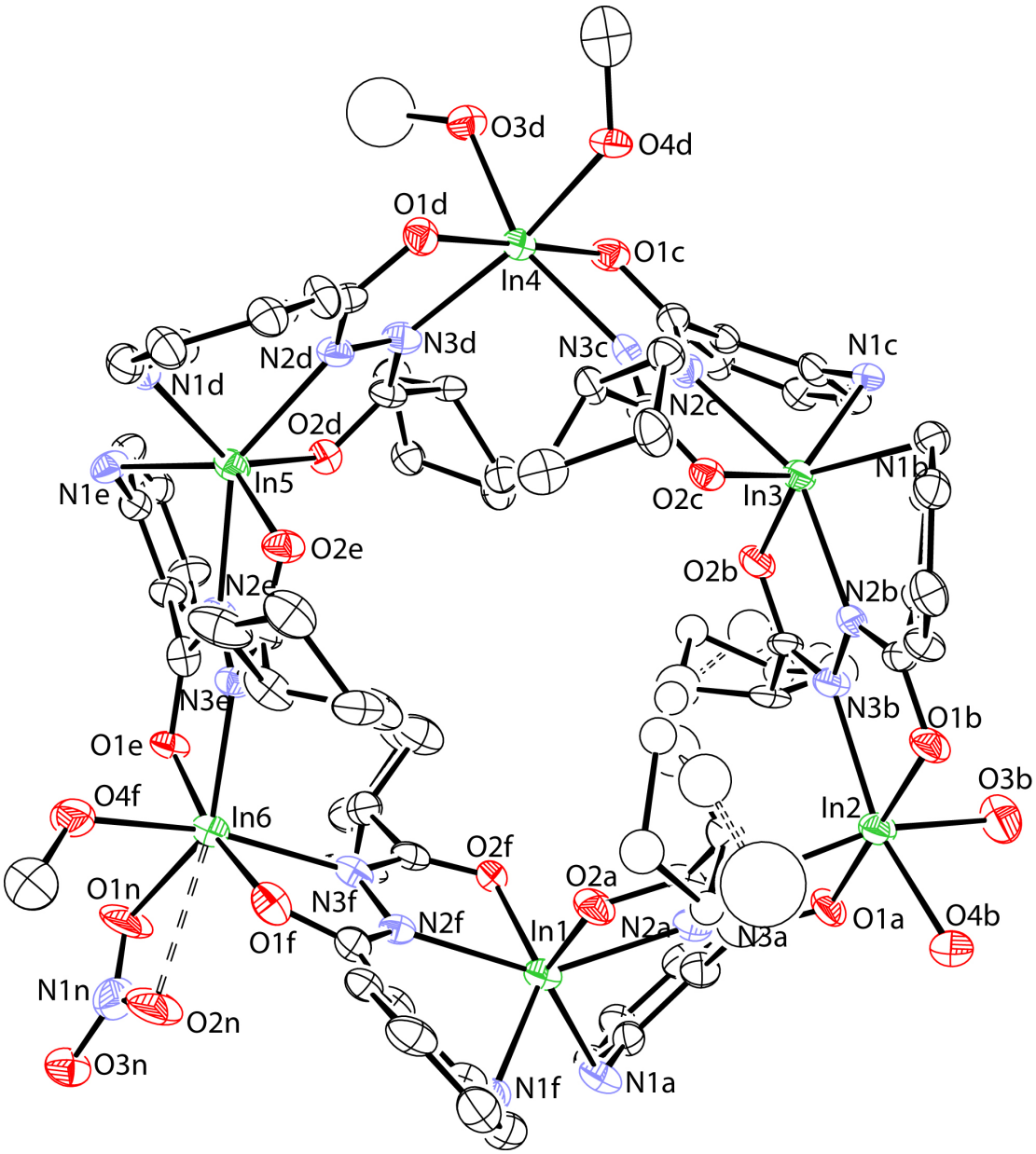

Figure S3. An ORTEP diagram of **1** with 20% of thermal ellipsoid probability displacement. Only metals and heteroatoms were labeled. For the sake of clarity all hydrogen atoms as well as counter ions were omitted.

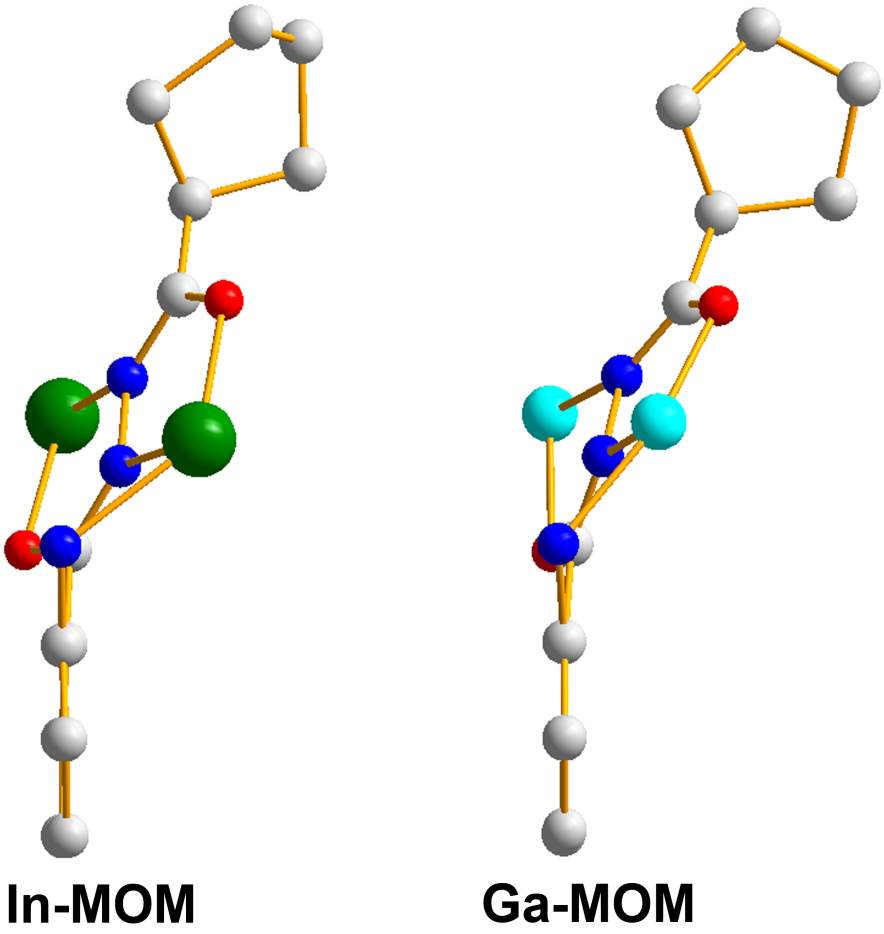

Figure S4. Conformations of the ligand in **1** and the Ga– MOM, $[Ga_8(H_2L^4)_8(NO_3)S_8](NO_3)_8$ (where, S is either MeOH or H_2O),[S1] showing different extents of the ligand planarity. Color codes: indium (green), gallium (cyan), oxygen (red), nitrogen (blue), and carbon (gray).

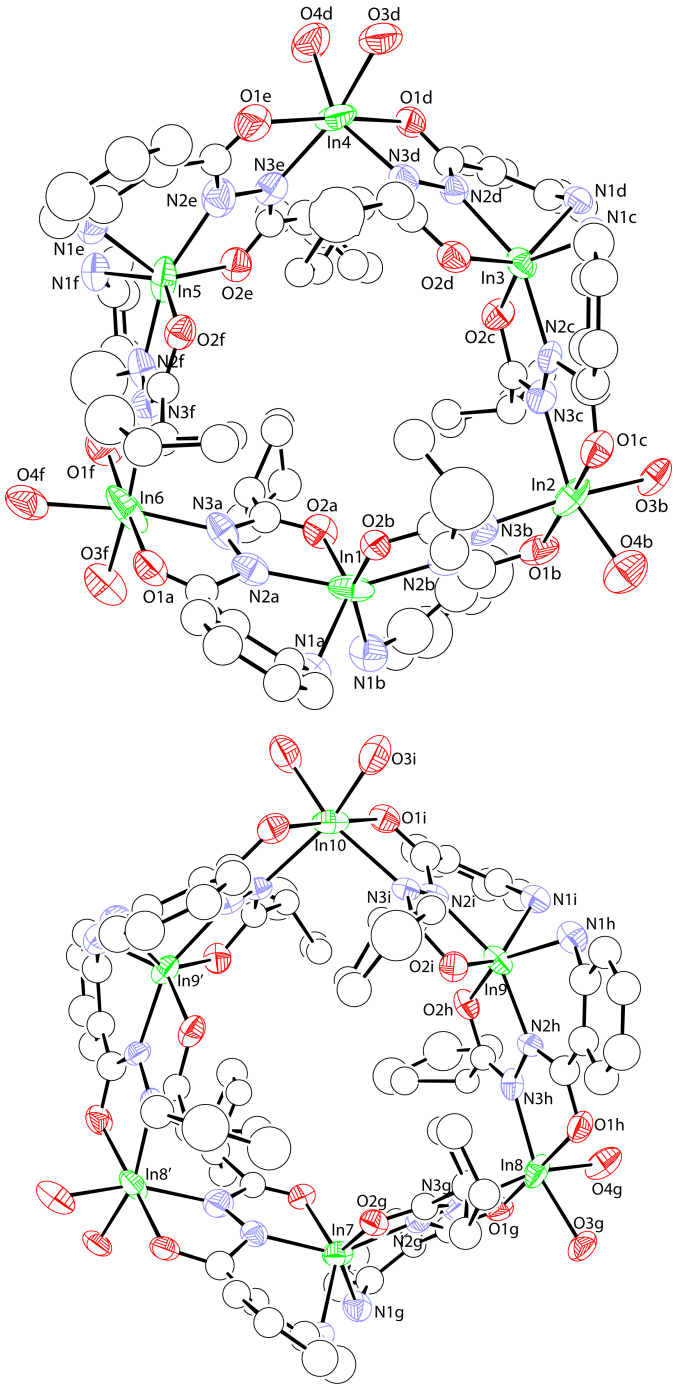

Figure S5. ORTEP diagrams of the In– MOMs in **2** with 20% of thermal ellipsoid probability displacement. Only metals and heteroatoms were labeled. For the sake of clarity all hydrogen atoms as well as the counter ions were omitted. (a) One In– MOM is on a crystallographic general position and (b) the other In– MOM is on the crystallographic twofold axis.

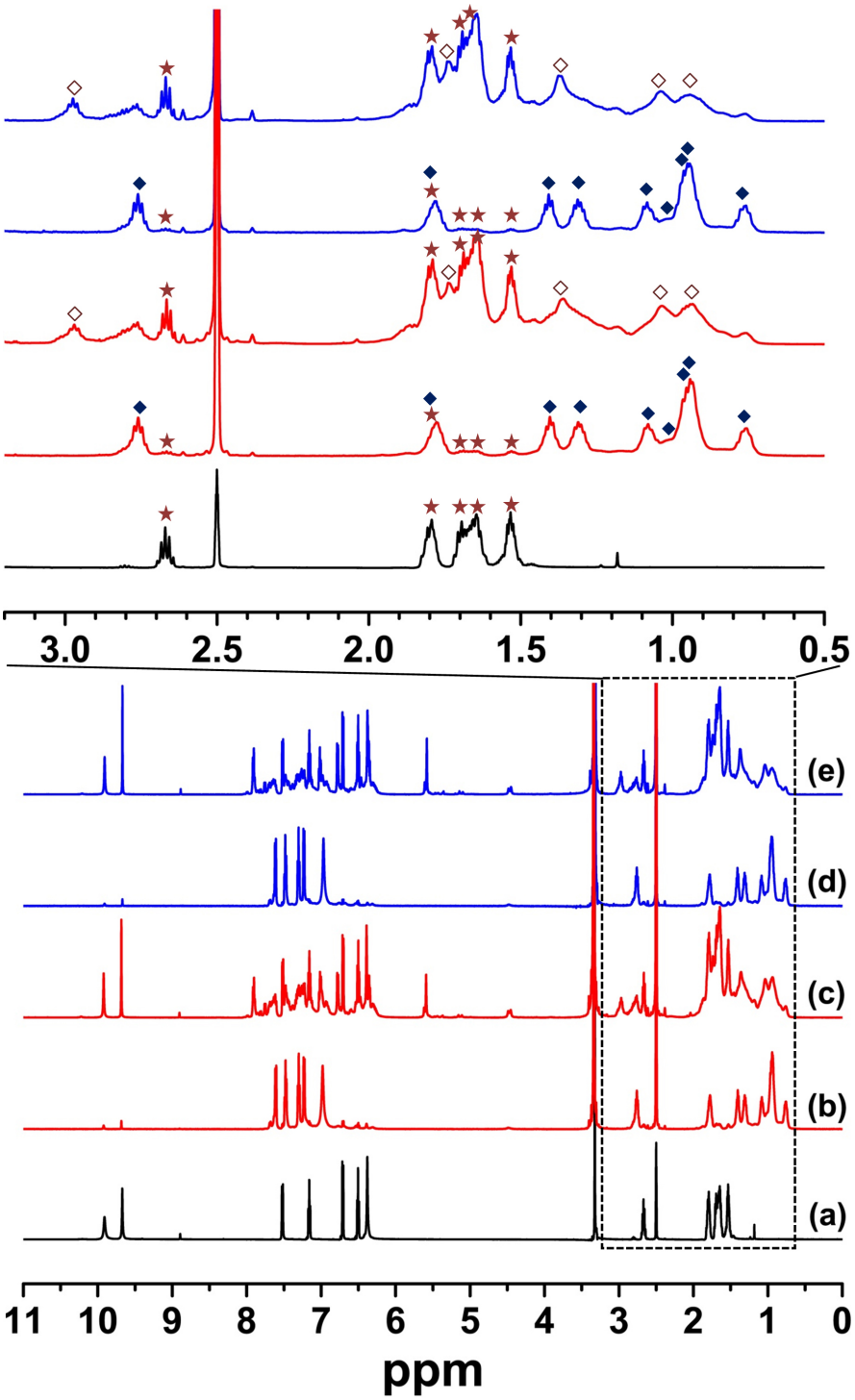

Figure S6. ^{1}H NMR spectra of the two different crystalline forms, **1** and **2**, in d_6-dmso with the expansion of 0.5–3.2 ppm range. ^{1}H NMR spectra of (a) H_4L[4], (b) **1** taken within 5 min after the preparation of the solution, (c) **1** taken at its equilibrium state, (d) **2** taken within 5 min after the preparation of the solution, and (e) **2** taken at its equilibrium state. ★ is for the free ligand, ◆ is for **2**, and ◇ is for the new species, **3**, in the equilibrium state.

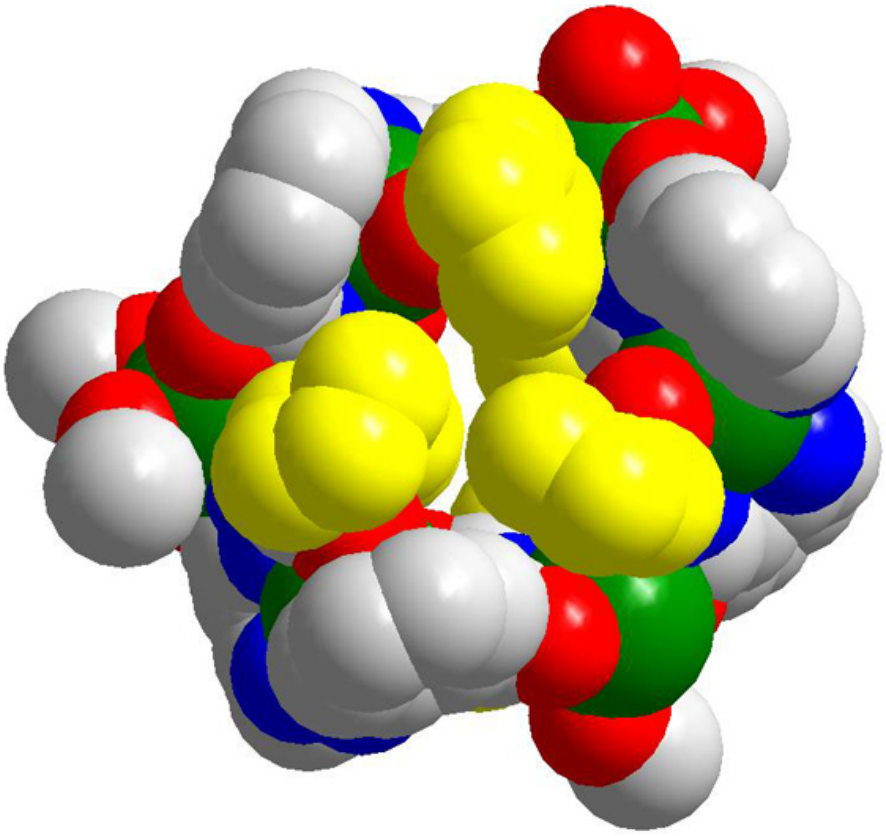

Figure S7. CPK diagram of **2**, where the cyclopentyl residues are represented in yellow. Color codes: cyclopentyl residue (yellow), indium (green), oxygen (red), nitrogen (blue), and carbon (gray).

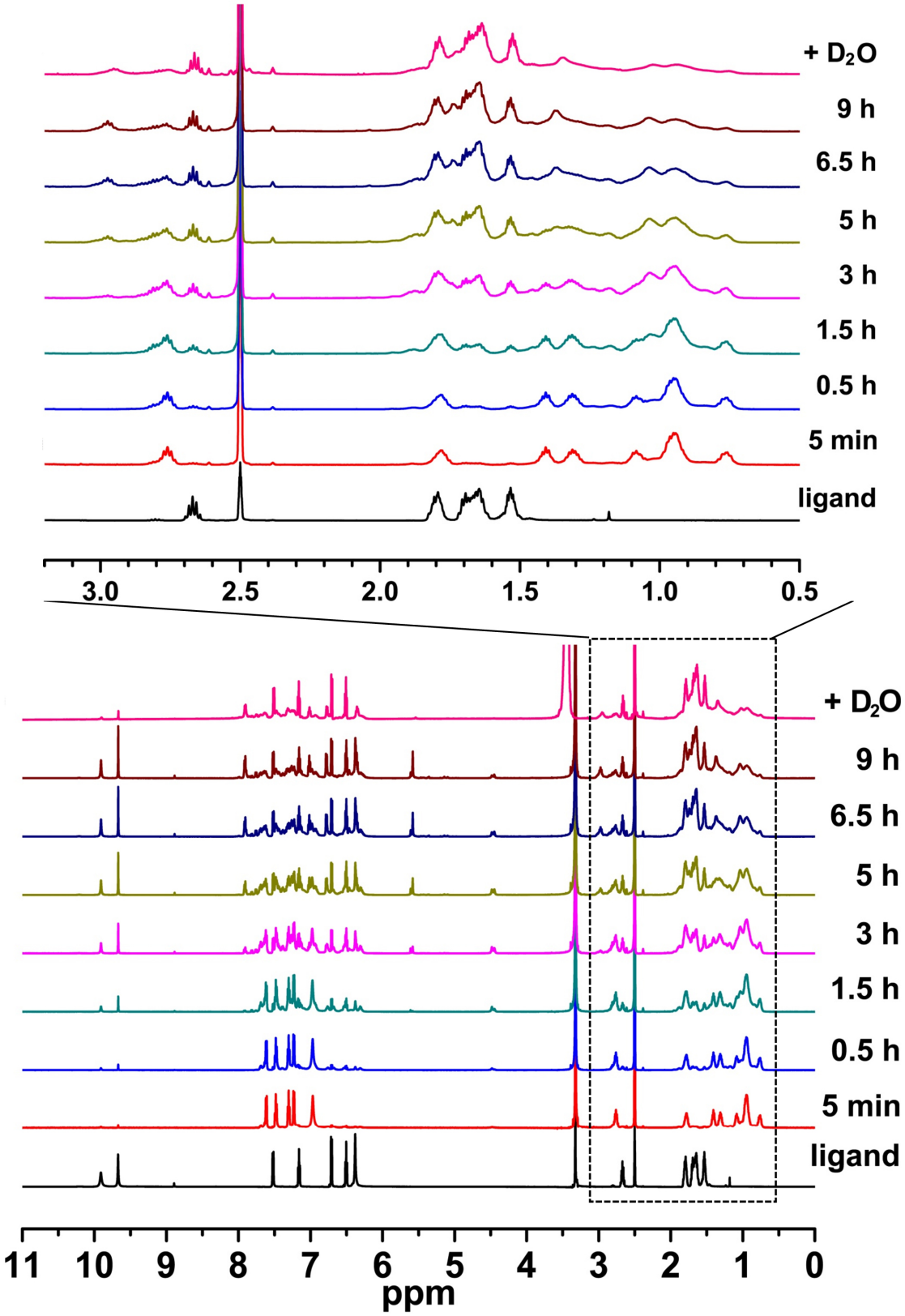

Figure S8. The time dependent ^{1}H NMR spectra of **2** in d_6-dmso with an expansion of 0.5–3.2 ppm range.

Table S1. Hydrogen bonds for **1** (Å and °).

D-H...A	d(D-H)	d(H...A)	d(D...A)	<(DHA)
N(1A)-H(1A1)...O(16N)#1	0.92	2.02	2.92(3)	166.6
N(1A)-H(1A2)...O(4S)#2	0.92	2.15	2.973(15)	147.7
N(1B)-H(1B1)...O(5N)#3	0.92	2.41	3.100(14)	132.3
N(1B)-H(1B2)...O(12N)	0.92	2.00	2.91(3)	175.2
N(1B)-H(1B2)...O(22N)	0.92	2.18	3.00(2)	148.0
N(1C)-H(1C1)...O(22N)	0.92	2.17	2.99(2)	147.9
N(1C)-H(1C2)...O(4N)#3	0.92	2.15	3.062(15)	171.2
N(1C)-H(1C2)...O(5N)#3	0.92	2.38	3.066(13)	131.6
N(1D)-H(1D1)...O(2N)#4	0.92	2.08	2.988(17)	170.6
N(1D)-H(1D2)...O(13N)	0.92	2.24	3.145(16)	169.0
N(1E)-H(1E1)...O(14N)	0.92	2.37	3.11(2)	136.4
N(1E)-H(1E2)...O(9N)	0.92	2.17	3.033(14)	154.9
N(1F)-H(1F1)...O(7N)#5	0.92	1.97	2.867(14)	165.9
N(1F)-H(1F2)...O(2S)#5	0.92	2.44	3.215(15)	141.6
N(1F)-H(1F2)...O(18N)#	0.92	2.45	3.093(19)	127.1
O(1S)-H(1S)...O(6N)	0.84	1.91	2.689(15)	153.3
O(2S)-H(2S)...N(1F)#4	0.84	2.59	3.215(15)	131.7
O(3S)-H(3S)...O(6N)#6	0.84	1.87	2.704(17)	173.4
O(4S)-H(4S)...O(2S)#4	0.84	2.05	2.854(17)	161.0

Symmetry transformations used to generate equivalent atoms:

#1 -x+0, y+0, z-1/2 #2 x-1, y, z #3 -x+1, -y, z

#4 x+1/2, -y+1/2, z #5 x-1/2, -y+1/2, z #6 -x+1, -y+1, z

Table S2. Bond angles (°) around the metal centers for **1** and $[Ga_8(H_2L^4)_8(NO_3)S_8](NO_3)_8$ (where S is either MeOH or H_2O)[S1].

O(2A)-In(1)-N(1A)	135.2(4)	O(2B)-In(3)-N(1B)	141.3(4)	O(2D)-In(5)-N(1D)	140.8(4)
O(2A)-In(1)-N(2A)	71.6(4)	O(2B)-In(3)-N(2B)	73.0(3)	O(2D)-In(5)-N(2D)	72.9(4)
O(2A)-In(1)-O(2F)	112.3(3)	O(2B)-In(3)-O(2C)	116.8(3)	O(2D)-In(5)-O(2E)	115.1(3)
O(2A)-In(1)-N(1F)	88.9(4)	O(2B)-In(3)-N(1C)	89.4(3)	O(2D)-In(5)-N(1E)	91.1(4)
O(2A)-In(1)-N(2F)	85.9(4)	O(2B)-In(3)-N(2C)	93.9(4)	O(2D)-In(5)-N(2E)	87.3(4)
N(1A)-In(1)-N(2A)	75.5(4)	N(2B)-In(3)-N(1B)	79.0(3)	N(2D)-In(5)-N(1D)	79.2(4)
O(2F)-In(1)-N(1A)	97.6(4)	O(2C)-In(3)-N(1B)	90.2(3)	O(2E)-In(5)-N(1D)	91.3(4)
N(1A)-In(1)-N(1F)	88.6(4)	N(1B)-In(3)-N(1C)	84.5(3)	N(1E)-In(5)-N(1D)	86.8(4)
N(2F)-In(1)-N(1A)	136.3(4)	N(2C)-In(3)-N(1B)	121.6(4)	N(2E)-In(5)-N(1D)	130.1(4)
O(2F)-In(1)-N(2A)	90.8(3)	O(2C)-In(3)-N(2B)	92.6(4)	O(2E)-In(5)-N(2D)	89.6(4)
N(1F)-In(1)-N(2A)	128.9(4)	N(2B)-In(3)-N(1C)	123.8(4)	N(2D)-In(5)-N(1E)	131.0(4)
N(2F)-In(1)-N(2A)	144.5(3)	N(2C)-In(3)-N(2B)	153.6(3)	N(2D)-In(5)-N(2E)	143.5(4)
O(2F)-In(1)-N(1F)	139.9(4)	O(2C)-In(3)-N(1C)	141.1(3)	O(2E)-In(5)-N(1E)	137.8(4)
O(2F)-In(1)-N(2F)	72.5(3)	O(2C)-In(3)-N(2C)	72.6(3)	O(2E)-In(5)-N(2E)	71.1(4)
N(2F)-In(1)-N(1F)	75.9(4)	N(2C)-In(3)-N(1C)	77.7(3)	N(2E)-In(5)-N(1E)	78.2(4)

The average bond angle deviation of the *mer*-tridentate/tridentate metal sites from ideal octahedral geometry: 24.6°

O(1A)-In(2)-N(3A)	75.5(4)	O(1C)-In(4)-N(3C)	74.9(3)	O(1E)-In(6)-N(3E)	75.3(3)
O(1B)-In(2)-O(1A)	179.8(4)	O(1D)-In(4)-O(1C)	178.4(3)	O(1E)-In(6)-O(1F)	170.5(3)
O(1A)-In(2)-O(3B)	82.3(4)	O(1C)-In(4)-O(3D)	83.0(3)	O(1E)-In(6)-O(1N)	70.8(4)
O(1A)-In(2)-O(4B)	94.5(4)	O(1C)-In(4)-O(4D)	93.9(3)	O(1E)-In(6)-O(4F)	93.0(4)
O(1A)-In(2)-N(3B)	106.0(4)	O(1C)-In(4)-N(3D)	102.4(3)	O(1E)-In(6)-N(3F)	102.2(4)
O(1B)-In(2)-N(3A)	104.7(4)	O(1D)-In(4)-N(3C)	105.1(3)	O(1F)-In(6)-N(3E)	96.8(4)
O(3B)-In(2)-N(3A)	157.1(4)	O(3D)-In(4)-N(3C)	155.3(3)	N(3E)-In(6)-O(1N)	143.6(4)
O(4B)-In(2)-N(3A)	91.6(4)	O(4D)-In(4)-N(3C)	84.2(3)	O(4F)-In(6)-N(3E)	83.9(4)
N(3A)-In(2)-N(3B)	96.6(4)	N(3D)-In(4)-N(3C)	100.7(3)	N(3F)-In(6)-N(3E)	102.1(4)
O(1B)-In(2)-O(3B)	97.4(4)	O(1D)-In(4)-O(3D)	97.2(3)	O(1F)-In(6)-O(1N)	118.0(4)
O(1B)-In(2)-O(4B)	85.5(4)	O(1D)-In(4)-O(4D)	87.7(3)	O(1F)-In(6)-O(4F)	91.3(4)
O(1B)-In(2)-N(3B)	74.0(4)	O(1D)-In(4)-N(3D)	76.0(3)	O(1F)-In(6)-N(3F)	74.0(4)
O(3B)-In(2)-O(4B)	84.5(5)	O(3D)-In(4)-O(4D)	86.5(3)	O(4F)-In(6)-O(1N)	84.8(5)
O(3B)-In(2)-N(3B)	94.9(4)	O(3D)-In(4)-N(3D)	94.7(3)	N(3F)-In(6)-O(1N)	97.9(4)
O(4B)-In(2)-N(3B)	159.3(4)	O(4D)-In(4)-N(3D)	163.6(4)	O(4F)-In(6)-N(3F)	164.6(4)

The average bond angle deviation of the *prop*-bidentate/bidentate metal sites from ideal octahedral geometry: 13.2°

Table S2. Continued.

O(2A)-Ga(1)-N(1A)	162.2(2)	O(2C)-Ga(3)-N(1C)	162.4(2)	O(2E)-Ga(5)-N(1E)	161.5(2)	O(2G)-Ga(7)-N(1G)	162.3(3)
O(2A)-Ga(1)-N(2A)	78.7(2)	O(2C)-Ga(3)-N(2C)	78.6(2)	O(2E)-Ga(5)-N(2E)	78.1(3)	O(2G)-Ga(7)-N(2G)	77.6(3)
O(2A)-Ga(1)-O(2H)	98.8(2)	O(1B)-Ga(3)-O(2C)	99.8(2)	O(2D)-Ga(5)-O(2E)	100.5(2)	O(2F)-Ga(7)-O(2G)	99.7(3)
O(2A)-Ga(1)-N(1H)	88.8(2)	O(2C)-Ga(3)-N(1B)	87.3(2)	O(2E)-Ga(5)-N(1D)	89.0(3)	O(2G)-Ga(7)-N(1F)	88.5(3)
O(2A)-Ga(1)-N(2H)	96.1(2)	O(2C)-Ga(3)-N(2B)	98.9(2)	O(2E)-Ga(5)-N(2D)	97.3(2)	O(2G)-Ga(7)-N(2F)	96.5(3)
N(2A)-Ga(1)-N(1A)	84.6(3)	N(2C)-Ga(3)-N(1C)	85.1(3)	N(2E)-Ga(5)-N(1E)	85.3(3)	N(2G)-Ga(7)-N(1G)	85.5(3)
O(2H)-Ga(1)-N(1A)	88.9(2)	O(1B)-Ga(3)-N(1C)	88.3(2)	O(2D)-Ga(5)-N(1E)	89.1(3)	O(2F)-Ga(7)-N(1G)	88.1(3)
N(1A)-Ga(1)-N(1H)	88.6(3)	N(1C)-Ga(3)-N(1B)	89.5(3)	N(1D)-Ga(5)-N(1E)	86.3(3)	N(1G)-Ga(7)-N(1F)	88.4(3)
N(2H)-Ga(1)-N(1A)	101.2(3)	N(2B)-Ga(3)-N(1C)	98.0(3)	N(2D)-Ga(5)-N(1E)	100.2(3)	N(2F)-Ga(7)-N(1G)	100.7(3)
O(2H)-Ga(1)-N(2A)	96.2(2)	O(1B)-Ga(3)-N(2C)	96.3(2)	O(2D)-Ga(5)-N(2E)	96.0(2)	O(2F)-Ga(7)-N(2G)	98.0(3)
N(2A)-Ga(1)-N(1H)	101.3(3)	N(2C)-Ga(3)-N(1B)	101.2(3)	N(2E)-Ga(5)-N(1D)	100.9(3)	N(2G)-Ga(7)-N(1F)	98.6(3)
N(2H)-Ga(1)-N(2A)	171.8(2)	N(2C)-Ga(3)-N(2B)	173.8(2)	N(2E)-Ga(5)-N(2D)	172.1(3)	N(2F)-Ga(7)-N(2G)	172.7(3)
O(2H)-Ga(1)-N(1H)	162.0(2)	O(1B)-Ga(3)-N(1B)	162.2(2)	O(2D)-Ga(5)-N(1D)	162.0(3)	O(2F)-Ga(7)-N(1F)	162.8(3)
O(2H)-Ga(1)-N(2H)	78.3(2)	O(1B)-Ga(3)-N(2B)	78.4(2)	O(2D)-Ga(5)-N(2D)	78.4(2)	O(2F)-Ga(7)-N(2F)	78.7(3)
N(2H)-Ga(1)-N(1H)	84.7(3)	N(2B)-Ga(3)-N(1B)	84.4(3)	N(2D)-Ga(5)-N(1D)	85.3(3)	N(2F)-Ga(7)-N(1F)	85.3(3)

The average bond angle deviation of the *mer*-tridentate/tridentate metal sites from ideal octahedral geometry: 9.7°

O(2B)-Ga(2)-O(3B)	87.5(2)	O(1D)-Ga(4)-O(3D)	88.3(3)	O(1F)-Ga(6)-O(3F)	85.8(3)	O(1H)-Ga(8)-O(3H)	87.5(3)
O(2B)-Ga(2)-O(4B)	91.6(3)	O(1D)-Ga(4)-O(4D)	91.7(3)	O(1F)-Ga(6)-O(4F)	92.8(4)	O(1H)-Ga(8)-O(4H)	91.5(3)
O(2B)-Ga(2)-N(3B)	78.8(2)	O(1D)-Ga(4)-N(3D)	78.6(2)	O(1F)-Ga(6)-N(3F)	79.5(3)	O(1H)-Ga(8)-N(3H)	79.2(3)
O(2B)-Ga(2)-O(1A)	178.1(2)	O(1C)-Ga(4)-O(1D)	178.7(2)	O(1F)-Ga(6)-O(1E)	176.7(3)	O(1H)-Ga(8)-O(1G)	178.4(3)
O(2B)-Ga(2)-N(3A)	101.7(3)	O(1D)-Ga(4)-N(3C)	101.9(3)	O(1F)-Ga(6)-N(3E)	102.6(3)	O(1H)-Ga(8)-N(3G)	100.7(3)
O(4B)-Ga(2)-O(3B)	86.0(3)	O(4D)-Ga(4)-O(3D)	86.8(3)	O(3F)-Ga(6)-O(4F)	86.3(3)	O(3H)-Ga(8)-O(4H)	86.2(3)
O(3B)-Ga(2)-N(3B)	166.2(3)	O(3D)-Ga(4)-N(3D)	166.7(3)	O(3F)-Ga(6)-N(3F)	164.4(3)	O(3H)-Ga(8)-N(3H)	165.8(3)
N(3A)-Ga(2)-N(3B)	96.2(2)	N(3D)-Ga(4)-N(3C)	95.9(3)	N(3F)-Ga(6)-N(3E)	97.5(3)	N(3H)-Ga(8)-N(3G)	97.0(3)
O(1A)-Ga(2)-O(3B)	91.3(2)	O(1C)-Ga(4)-O(3D)	92.3(3)	O(1E)-Ga(6)-O(3F)	91.1(3)	O(1G)-Ga(8)-O(3H)	91.0(3)
O(3B)-Ga(2)-N(3A)	88.3(2)	O(3D)-Ga(4)-N(3C)	88.8(3)	O(3F)-Ga(6)-N(3E)	90.7(3)	O(3H)-Ga(8)-N(3G)	90.2(3)
O(4B)-Ga(2)-N(3B)	92.5(3)	O(4D)-Ga(4)-N(3D)	91.4(3)	O(4F)-Ga(6)-N(3F)	89.3(3)	O(4H)-Ga(8)-N(3H)	89.3(3)
O(1A)-Ga(2)-O(4B)	86.8(3)	O(1C)-Ga(4)-O(4D)	87.2(3)	O(1E)-Ga(6)-O(4F)	86.0(3)	O(1G)-Ga(8)-O(4H)	87.9(3)
O(4B)-Ga(2)-N(3A)	165.3(3)	O(4D)-Ga(4)-N(3C)	165.6(3)	O(4F)-Ga(6)-N(3E)	164.0(4)	O(4H)-Ga(8)-N(3G)	167.2(3)
O(1A)-Ga(2)-N(3B)	102.3(2)	O(1C)-Ga(4)-N(3D)	100.7(3)	O(1E)-Ga(6)-N(3F)	103.5(3)	O(1G)-Ga(8)-N(3H)	102.3(3)
O(1A)-Ga(2)-N(3A)	79.9(2)	O(1C)-Ga(4)-N(3C)	79.3(2)	O(1E)-Ga(6)-N(3E)	78.4(3)	O(1G)-Ga(8)-N(3G)	79.8(2)

The average bond angle deviation of the *prop*-bidentate/bidentate metal sites from ideal octahedral geometry: 8.2°

Table S3. Bond distances (Å) around the metal centers for **1** and $[Ga_8(H_2L^4)_8(NO_3)S_8](NO_3)_8$ (where S is either MeOH or H_2O)[S1].

In(1)-O(2A)	2.139(8)	In(3)-O(2B)	2.131(9)	In(5)-O(2D)	2.128(8)
In(1)-N(1A)	2.245(11)	In(3)-N(1B)	2.219(10)	In(5)-N(1D)	2.235(9)
In(1)-N(2A)	2.288(10)	In(3)-N(2B)	2.219(10)	In(5) -N(2D)	2.205(10)
In(1)-O(2F)	2.152(8)	In(3)-O(2C)	2.144(8)	In(5)-O(2E)	2.125(9)
In(1)-N(1F)	2.214(10)	In(3)-N(1C)	2.300(9)	In(5)-N(1E)	2.240(10)
In(1)-N(2F)	2.251(10)	In(3)-N(2C)	2.210(9)	In(5)-N(2E)	2.205(11)
In(2)-O(1A)	2.146(8)	In(4)-O(1C)	2.115(9)	In(6)-O(1E)	2.096(9)
In(2)-N(3A)	2.208(11)	In(4)-N(3C)	2.212(10)	In(6)-N(3E)	2.237(10)
In(2)-O(1B)	2.162(8)	In(4)-O(1D)	2.122(8)	In(6)-O(1F)	2.132(9)
In(2)-O(3B)	2.158(10)	In(4)-O(3D)	2.183(8)	In(6)-O(1N)	2.407(10)
In(2)-O(4B)	2.169(11)	In(4)-O(4D)	2.179(9)	In(6)-O(4F)	2.162(10)
In(2)-N(3B)	2.215(10)	In(4)-N(3D)	2.222(10)	In(6)-N(3F)	2.215(11)
avg. In-O	**2.16(7)**	**avg. In-N**	**2.23(3)**		

Ga(1)-O(2A)	1.960(5)	Ga(3)-O(1B)	1.963(5)	Ga(5)-O(2D)	1.950(5)	Ga(7)-O(2F)	1.959(6)
Ga(1)-N(1A)	2.088(6)	Ga(3)-N(1B)	2.092(6)	Ga(5)-N(1D)	2.074(7)	Ga(7)-N(1F)	2.090(7)
Ga(1)-N(2A)	1.997(6)	Ga(3)-N(2B)	2.023(7)	Ga(5)-N(2D)	2.024(7)	Ga(7)-N(2F)	2.012(7)
Ga(1)-O(2H)	1.977(5)	Ga(3)-O(2C)	1.971(5)	Ga(5)-O(2E)	1.967(5)	Ga(7)-O(2G)	1.967(6)
Ga(1)-N(1H)	2.101(7)	Ga(3)-N(1C)	2.087(6)	Ga(5)-N(1E)	2.081(7)	Ga(7)-N(1G)	2.082(7)
Ga(1)-N(2H)	1.980(6)	Ga(3)-N(2C)	1.996(6)	Ga(5)-N(2E)	2.006(7)	Ga(7)-N(2G)	2.015(7)
Ga(2)-O(1A)	1.950(5)	Ga(4)-O(1C)	1.922(6)	Ga(6)-O(1E)	1.948(8)	Ga(8)-O(1G)	1.934(6)
Ga(2)-N(3A)	2.037(6)	Ga(4)-N(3C)	2.081(7)	Ga(6)-N(3E)	2.088(7)	Ga(8)-N(3G)	2.064(7)
Ga(2)-O(2B)	1.917(6)	Ga(4)-O(1D)	1.955(6)	Ga(6)-O(1F)	1.920(8)	Ga(8)-O(1H)	1.931(6)
Ga(2)-O(3B)	2.017(5)	Ga(4)-O(3D)	2.000(6)	Ga(6)-O(3F)	2.008(6)	Ga(8)-O(3H)	1.985(6)
Ga(2)-O(4B)	1.975(6)	Ga(4)-O(4D)	1.971(6)	Ga(6)-O(4F)	2.019(7)	Ga(8)-O(4H)	1.996(6)
Ga(2)-N(3B)	2.075(6)	Ga(4)-N(3D)	2.067(6)	Ga(6)-N(3F)	2.052(7)	Ga(8)-N(3H)	2.049(6)
avg. Ga-O	**1.97(3)**	**avg. Ga-N**	**2.05(4)**				

Reference

S1. Park, M.; John, R. P.; Moon, D.; Lee, K.; Kim, G. H.; Lah, M. S. *Dalton Trans.* **2007**, 5412.